NEUTRON RADIOSCOPY AT THE SLOWPOKE-2 FACILITY AT RMC

FOR THE INSPECTION OF CF-18 FLIGHT CONTROL SURFACES

T. R. Chalovich

Department of Chemistry and Chemical Engineering, Royal Military College of Canada, Kingston, Ontario, Canada K7K 7B4
chalovich-t@rmc,ca

Abstract

Recent developments in Charged Coupled Device (CCD) cameras have made real and semi-real time neutron radioscopy an affordable and reasonable alternative to neutron radiography utilising film techniques. Developing and analysing the capability of a Neutron Radioscopy System (NRS) at the SLOWPOKE-2 Facility at Royal Military College (RMC) was carried out with the result that neutron radioscopy was determined to be feasible for use in the detection of water ingress in CF-18 flight control surfaces.

1. Introduction

Neutron radiography is a Non-destructive Testing (NDT) technique which is complementary to X and Gamma radiography. Neutron radiography utilises neutrons, which interact with nuclei of atoms rather than with the orbital electrons as does X or Gamma radiation. A comparison of the mass attenuation coefficient for most of the elements for thermal neutrons and X-radiation (Figure 1) shows that each nuclide has its own characteristic neutron cross section which shows no pattern compared to the increasingly uniform attenuation with mass number for X and Gamma radiation. In fact, there is a slight reverse or complementary trend towards light elements for neutrons. The major advantage of neutron radiography is its ability to see light elements such as contained in corrosion and water. The energy spectrum, composition and quantity of neutrons in the beam at the image plane will determine image quality and exposure time.

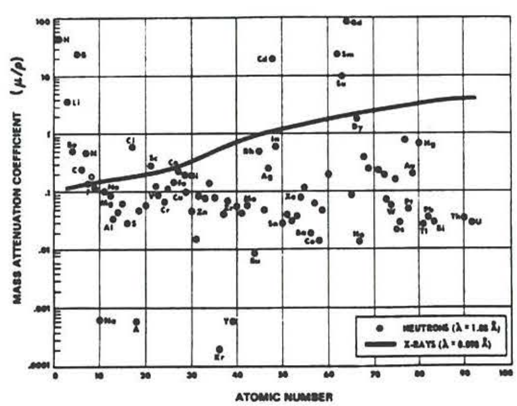

Figure 1 - Mass Attenuation Coefficients as a Function of Atomic Number[1]

Neutron radioscopy does not utilise film but rather a Vidicon video camera with screen intensifiers or a Charged Coupled Device (CCD) camera with a scintillation screen to record the image. The image is stored in a digital format on a computer for viewing and digital enhancement purposes. The major disadvantage of neutron radioscopy is poor image resolution while the advantages include good image contrast, reduced exposure time, very good image linearity and the ability to manipulate image data. A typical configuration for neutron radioscopy is shown in Figure 2.

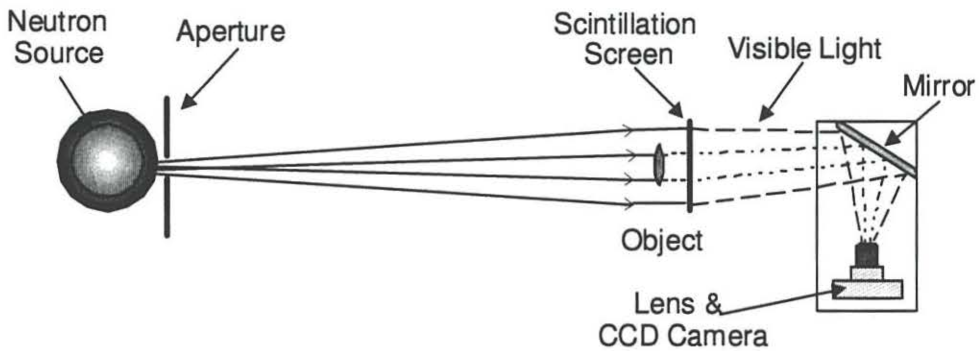

Figure 2 - Neutron Radioscopy Configuration

In radioscopy, neutrons interact (by either absorption or scatter) with an object, reducing the amount of neutrons that hit the scintillating screen. Therefore, the screen is not exposed in this area, but the remaining area of the scintillating screen will be luminous. The radiographer will view the area associated with the object as a darker shade of grey compared to the surrounding area. Essentially, a positive image, rather than a negative one, is directly obtained. Figure 3 is a drawing illustrating the results of radiography (using film) and radioscopy (using a scintillating screen).

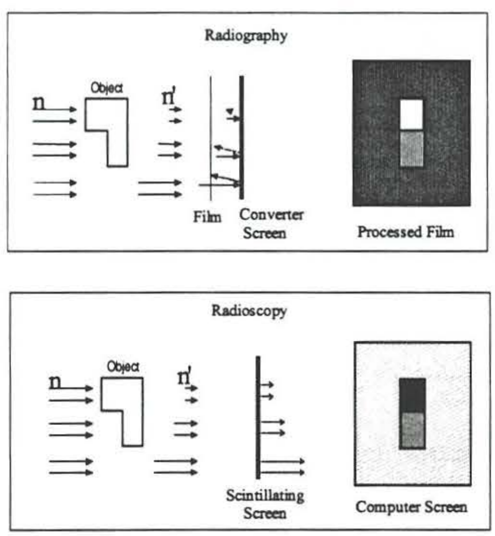

Figure 3 – Radiography and Radioscopy Image Formation

Using a CCD camera was first applied to neutron radioscopy in 1990.[2] Advancements in CCD camera and cooling technology have made the use of CCD cameras both affordable and practical. There are two phases in the installation of a CCD camera system. The first phase is the assembly of the hardware, which includes the CCD camera, mirror, lens, scintillation screen, and a light-tight enclosure. The second phase is the testing of the CCD camera system to determine its capabilities and performance. Testing of the system includes quantifying the system's resolution, optimising the exposure time, quantifying the neutron-scintillation screen interaction and quantifying the results from images taken with actual aircraft flight control surfaces.

In the recent past, a small sample of Canadian Military F-18 flight control surfaces were inspected using several different NDT techniques. The goal of the inspection was to determine the extent of water ingress and then determine the appropriate NDT methods for detecting water ingress. Neutron radiography was found to be the best;[3] however, this inspection technique tended to be labour and time intensive. The goal in developing a CCD camera system was to reduce the inspection time of the flight control surfaces without sacrificing the ability to detect small amounts of water inside.

2. Equipment and Methods

Two different nuclear reactors were used as a neutron source in order to determine the effects on the image of different neutron fluxes. The first neutron source used was the 20 kW_t research reactor in the SLOWPOKE-2 Facility at RMC. For neutron radiography/radioscopy, the reactor, which normally operates at half power (10 kW_t), produces a nominal neutron flux of 5.0×10^5 n/cm^2 s outside the reactor core and produces 2.0×10^4 n/cm^2 s at the image plane.[4] The Neutron Beam Tube (NBT) is circular in cross section, tilted 8.5° from vertical and has a measured L/D of approximately 100.[5] At the inlet of the NBT, the neutron beam passes vertically into a series of beam stops: through the bottom one (on top of which the object to be radiographed is positioned) and into the middle and top beam stop in which the scintillation screen and CCD camera are located. This arrangement is termed the Neutron Radioscopy System (NRS), Figure 4.

The second neutron source was the Breazeale reactor facility at Pennsylvania State University (referred to as Penn State). This facility is capable of producing a maximum power of 1 MW_t. For the experiments, the reactor was set to 1, 10, 100 kW_t which equate to a neutron flux level at the image plane of 3.0×10^4 n/cm^2 s (calculated), 3.0×10^5 n/cm^2 s (calculated), and 3.0×10^6 n/cm^2 s (measured),[6] respectively. The beam tube has a circular cross section, is horizontal and has an L/D ratio of 34.

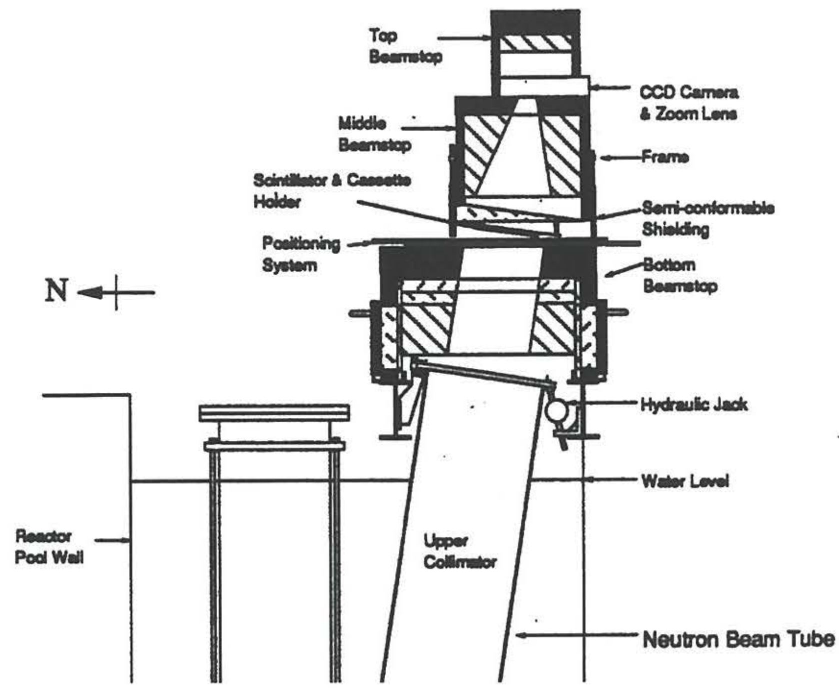

Figure 4 - NRS at RMC

The camera system consisted of a 431.8 mm (17 in.) x 431.8 mm (17 in) aluminium backed $^{6}LiF:ZnS:Cu$ scintillating screen, an Apogee AP7 CCD camera with a SITe502 CCD sensor, a front surface mirror with adjusting mechanism, a Vivitar AF-SC 28-70 mm, F3.5 zoom lens, an Apogee video capture board and a 200 MHz computer running Windows 98. The SITe502 CCD is a back lit, full frame CCD chip with an array size of 512 x 512 and a pixel size of 24μm. The CCD camera, cooling unit, mirror and mirror adjuster are housed in a self-contained unit and is thermoelectrically cooled to a -30°C working temperature. For the experiment at Penn State, the same geometrical arrangement of the scintillation screen and CCD camera were temporally configured by designing an aluminium rectangular and trapezoidal enclosure that was dimensionally identical to the middle beam stop at RMC. Image acquisition was accomplished with "Image Pro Plus" and image analysis was completed with "IP Lab Spectrum –Scientific Imaging Software for Macintosh". All image analysis was done on an Apple Macintosh Computer, Model 8500, as recommended by the software vendor.

A digital image is constructed from a 3D matrix comprising values indicating the x and y location and intensity level for every pixel location in an image. A histogram is a graph that compiles the intensity data from an image into a particular format. By convention, the y-axis corresponds to the amount of pixels per intensity interval and the x-axis is the intensity scale, from 0 (black) to 65536 (white). The x-axis is divided into sequentially grouped intensity intervals. An intensity interval can have a range of values from one to a maximum of 256.

For neutron radioscopy, the component of interest is the CF-18 Hornet's rudders, which have indicated the greatest potential for water ingress into the honeycomb structure.[7]

The covering on the rudder is carbon graphite (as indicated in Figure 5) and has an aluminium six sided honeycomb material used as the core of the component. The flight control surfaces have structural pieces that allow for hinge connection and strengthening of the trailing edge which also completely seal the honeycomb (made from 5052 or 5056 aluminium alloy) inside the component.

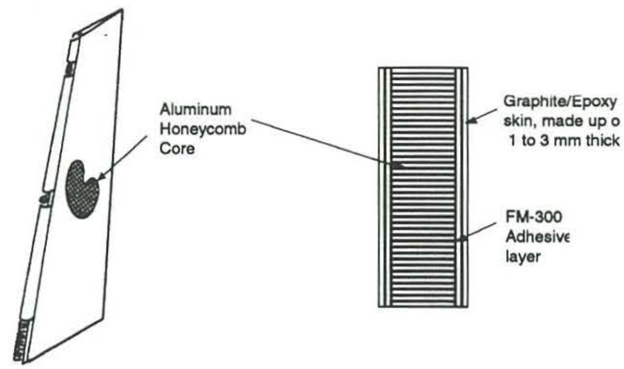

Figure 5 - Construction of a CF-18 Rudder

A CF-18 Rudder, serial number 0241, was inspected as per technique MC-188-311-NRT (revision 1) utilising radioscopy instead of radiography techniques[8]. The RMC NRS is capable of mapping all 8 positions of the rudder, but only exposure 5 will be analysed.

To understand the results of the neutron radioscopy performed on the CF-18 rudder, a basic knowledge of the internal structure is required. A neutron radioscopy image of a serviceable section of a rudder with its components labelled is shown in Figure 6. Table 1 lists the components corresponding to the capital letters in Figure 6.

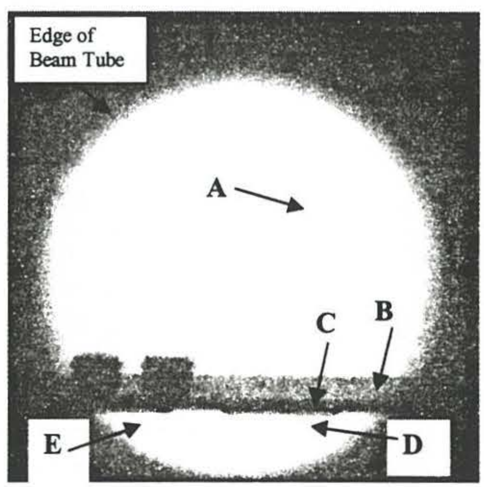

Figure 6 – Exposure 2 of Rudder from Penn State

Since the neutron beam at Penn State did not completely cover the entire area of the scintillation screen, all RMC images were cropped so that the images could be compared. Only the data inside the circle were used in the histograms as the data associated with the dark area outside the circle were excluded from the histograms. All images are presented in a format similar to Figure 6 and contain similar internal components as indicated in Table 1.

Table 1 – Internal Components of CF-18 Rudder

Letter	Component
A	Aluminium Honeycomb pattern From FM300 adhesive
B	Porous Adhesive – Connects honeycomb to main spar
C	Main Spar – Aluminium material
D	10/32 Steel Anchor Nuts (four in total)
E	0.050 inch Aluminium Sheet – Fairing support

3. Results and Discussion

For this paper, the exposure 5 position of the CF-18 rudder being inspected was used to produce images at RMC with the reactor at 10 kW_t and at Penn State with the reactor at 100 kW_t. The images were then processed and are described below.

Figure 7 shows a series of images taken at RMC of Exposure 5. The original image (a) is without any data manipulation and the second image (b) had the contrast and brightness manipulated to make the original image visible. The last image (c) has had a 2 x 2 Erosion filter applied to the original image and then the brightness and contrast were manipulated.

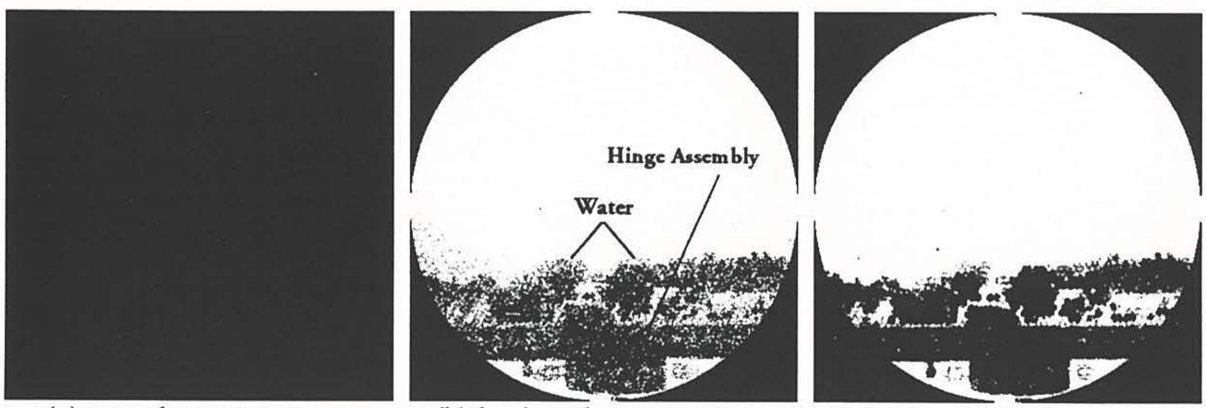

(a) no enhancements (b) basic enhancements (c) advanced enhancements

Figure 7- Sequence of Exposure 5 images taken at RMC

Although not visible in Figure 7a, there are some white spots indicating gamma contamination or system noise. Figure 7b has very little definition, as some of the individual components shown in Figure 6 are not clearly distinguishable but water is indicated, as is the hinge assembly. Water ingress and its location in this area was previously known from neutron radiography. In Figure 7b and c, water ingress is visible and the pattern of water is identical to known images of this area. Figure 7c also indicates clearer details such as the main spar, porous adhesive and the anchor nuts.

The histogram associated with the original image in Figure 7a of exposure 5 taken at RMC is shown in Figure 8. Thresholding was applied to the image to identify the features on the curve and are indicated on the histogram.

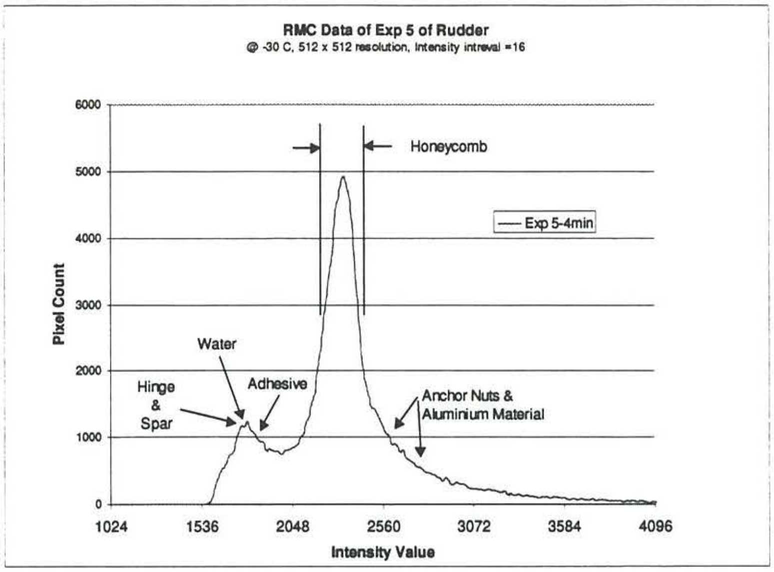

Figure 8 - Histogram of Exposure 5 from RMC (10 kW_t)

The intensity values of the graph in Figure 8 are in the low thousands and therefore the original image is black as previously seen in Figure 7a. The intensity value does not have a large range, from 1536 to approximately 3500 values, producing an image with a small dynamic range, which reduces image contrast between components as shown in Figure 7c.

An image of Exposure 5 was taken at Penn State with the reactor at 100 kW_t, Figure 9a and b. At this power setting, the flux at the image plane was two magnitudes greater than available at the RMC NRS. Due to the higher flux values, the only enhancement required was a small change to the contrast and brightness to produce the image in Figure 9b.

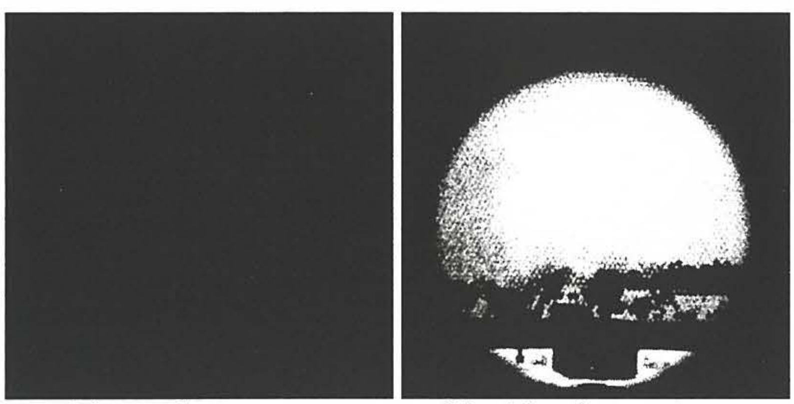

(a) no enhancement (b) with enhancements

Figure 9 - Sequence of Exposure 5 images taken at Penn State, 100 kW_t

Unlike the previous unaltered images, the rudder components are visible and, with only a small amount of contrast and brightness adjustment, a good image of Exposure 5 can be seen in Figure 9, b. All internal components show good definition and dynamic intensity range.

The applicable histogram for Figure 9a with labels indicating the major components of the rudder is presented in Figure 10.

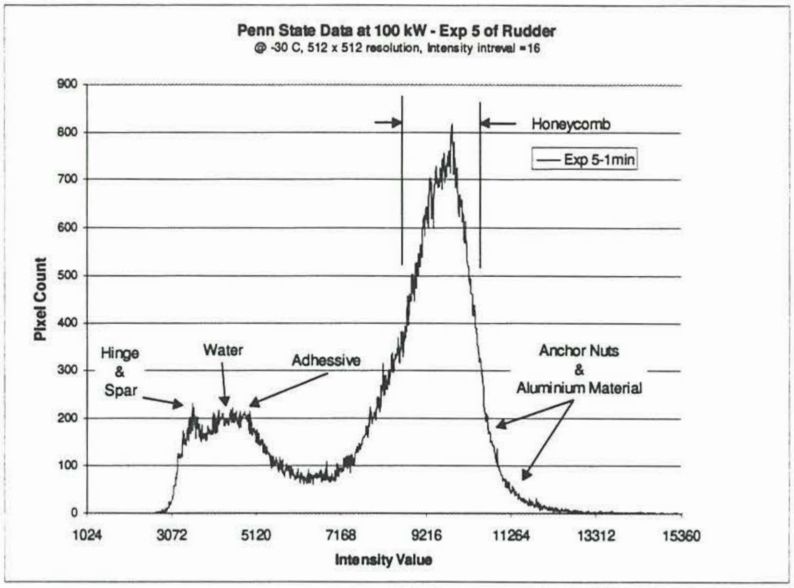

Figure 10 -Histogram of Exposure 5 from Penn State at 100 kW$_t$

This histogram has a very large intensity scale ranging from approximately 3000 to 12000. Since the histogram spans past the intensity value of 10,000, the image should be visible as can be seen in Figure 9a. The large dynamic range of this histogram should translate to significant differences in intensity values for given internal components of the rudder, which can be seen in Figure 9b.

The image produced at a 100 kW$_t$ power setting in Figure 9 has the best definition and largest range of intensities compared to the other images taken at RMC and Penn State (at lower power settings). Both images from RMC (10 kW$_t$) and Penn State (at 100 kW$_t$) show the internal components of the rudder and the water ingress in Figure 11. Due to the clarity of the images produced from the Penn State reactor at 100 kW$_t$, these images can be used as a comparison standard.

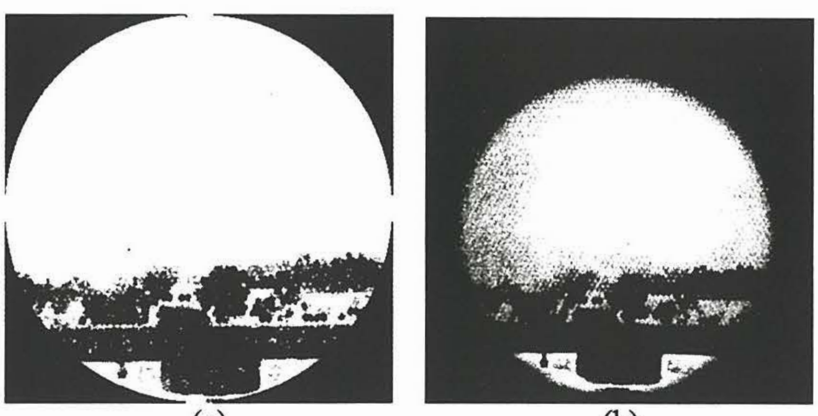

(a) (b)

Figure 11 - Exposure 5 from (a) RMC at 10 kW$_t$, and (b) Penn State at 100 kW$_t$

Plotting normalised histograms of Exposure 5 for RMC at 10 kW$_t$ with an exposure time of 4 minutes and Exposure 5 from Penn State at 100 kW$_t$ with an exposure time of 1 minute produced results shown in Figure 12. Both sets of data were normalised to the centroid of the honeycomb peak.

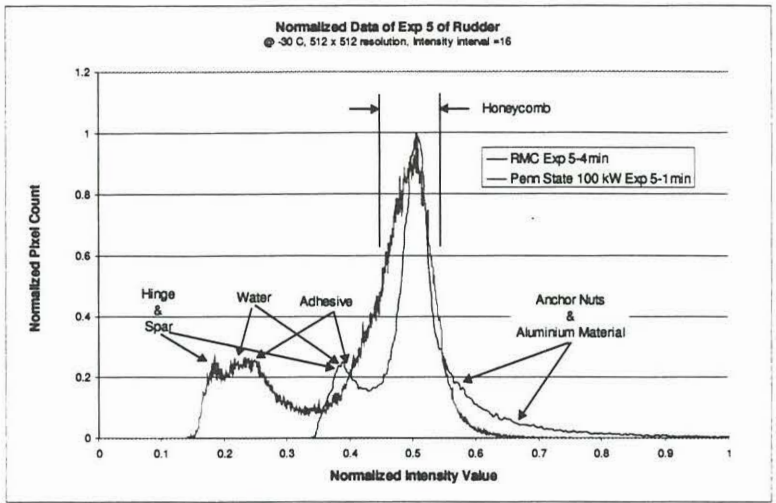

Figure 12 - Normalised Graph at Two Different Power Settings

Normalising the data allowed a direct comparison between the two graphs and compensated for the large variation of values of the pixel count and intensities. The goal in normalising the data was to confirm that both images produced similar shapes and features that related to the internal components of the rudder. Although the histogram graphs are not identical, the shapes are similar and features on the graph do relate to specific items in the images. The difference between the two graphs shows that the histogram from the image taken at Penn State uses a good percentage of the intensity scale. The curve of the histogram from the image taken at RMC is compressed on the left side of the peak and elongated on the right side of the peak relative to the other histogram. Overall, the image taken at RMC contains all the required data to produce an image that is capable of indicating the honeycomb pattern, main spar, porous adhesive, anchor nuts, aluminium structure and water ingress.

4. Conclusion

A neutron radioscopy system using a CCD camera and scintillation screen has been installed, developed and tested at the SLOWPOKE-2 Facility at RMC. The main purpose of the camera installation was to inspect CF-18 flight control surfaces for water ingress into the honeycomb structure using neutron radioscopy. It has been shown that the low flux values (2.0×10^4 n/cm^{2}s) produced by the SLOWPOKE-2 Facility at the image plan are sufficient to indicate water ingress into the flight control surface with image enhancements. As well as water ingress, internal components of the rudder can also be identified when simple image enhancement techniques are applied. The quality of the images taken at RMC were compared to images taken at Penn State facility which had flux levels at the image plane two magnitudes larger. Images produced at the Penn State facility with the same camera system showed larger intensity differences between internal components and better quality images overall, at a quarter of the exposure time. However, the SLOWPOKE-2 Facility at RMC has a neutron radioscopy CCD system that is sufficiently capable of detecting water ingress in CF-18 flight control surfaces.

---

[1] Standard Practices for Thermal Neutron Radiography of Materials, ASTM E 748-95, American Society for Testing and Materials, PA, USA, 1995.

[2] H.Kobayasi, Neutron Radiography, 3, Kluwer, pg. 421, 1990.

[3] Lepine B, McRae K, Progress in the Non-Destructive Evaluation of CF-18 Composite Flight Controls For Water Ingress and Related Damage, DCIEM Report No. 98 –TM-44, 1998

[4] M. Bickerton, Development of Improved Techniques for the Neutron Radiography of CF188 Flight Control Surfaces, Department of Chemistry and Chemical Engineering, Royal Military College of Canada, Kingston Ontario, 1998.

[5] W.J. Lewis, L.G.I. Bennett, C.T. Kirby, Enhancement to Neutron Radiology Facility at the SLOWPOKE-2 Facility at RMC, 5 World Conference on Neutron radiography, Berlin, 1996.

[6] J.S. Brenizer. D.E. Hughes, M.E. Bryan, R. Gould, T.L. Flinchbaugh, C.F. Sears, Recent Improvements to the Pennsylvania State University's Neutron Radiography Facility. 1998

[7] Lepine B, McRae K, Progress in the Non-Destructive Evaluation of CF-18 Composite Flight Controls For Water Ingress and Related Damage, DCIEM Report No. 98 –TM-44, 1998

[8] O. Francescone, W. Lewis, MC-188-311-NRT (Rev 1), Canadian Armed Forces N-Ray Inspection, Royal Military College, Kingston, Canada, Aug 25 1999